# ChemComm

Accepted Manuscript


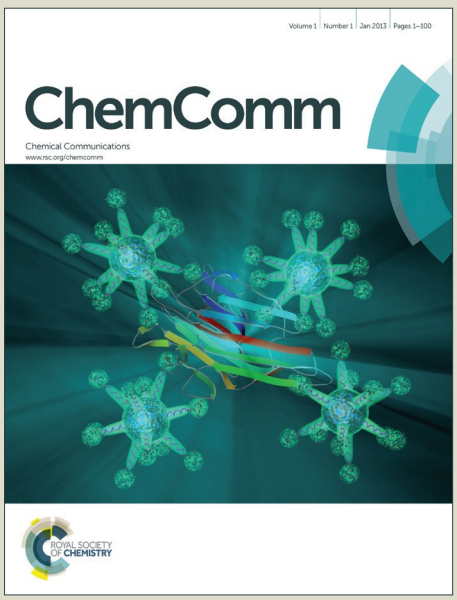





ROYAL SOCIETY OF CHEMISTRY

www.rsc.org/chemcomm

Journal Name

COMMUNICATION

# Ternary cooperative assembly—polymeric condensation of photoactive viologen, phosphonate-terminated dendrimers and crystalline anatase nanoparticles

Received 00th January 20xx,
Accepted 00th January 20xx

DOI: 10.1039/x0xx00000x

www.rsc.org/

Nadia Katir,[a] Younes Brahmi,[b] Jean Pierre Majoral,[c] Mosto Bousmina,[a] and Abdelkrim El Kadib.[a,*]

**Photo-active viologen fragments were covalently embedded within the material framework during the self-assembly and sol-gel polymerisation of phosphonate-terminated dendrimers and soluble titanium-oxy-species. The resulting porous anisotropic phosphonate-bridged-crystalline anatase materials serve as new hosts to disperse and stabilize small gold nanoparticles.**

In line with the rising interest for mesoporous materials, the last two decades have witnessed an extensive body of work revolving around the design of novel phosphonate-bridged-transition metal oxide materials.[1] This particular interest is rooted in the versatility and high performance of these materials compared to the early-explored organosilicates analogues. The inertness of the silica and its hydrolytic instability[2] illustrate some potential drawbacks of siliceous materials that stimulate the search for valuable alternatives. Paradoxically, organophosphonate-bridged-metal oxides display many practical advantages, among them: i) great stability of P-O-M bonds (M = Ti, Zr, Al, Sn, V) at the organic-inorganic hybrid interface, ii) highest chemo-, opto- and photo-reactivity of transition metal oxides, and iii) additional benefits attributed to the presence of phosphorus elements including inherent acidity, metal ligation ability and anchoring sites for further functionalization.[3] This results in a broad spectrum of utilisation. Consequently, these building-blocks are prominent contenders in multifunctional hybrid material synthesis.

In practical terms, there are two synthetic methodologies enabling access to these materials: i) the post-grafting of an organophosphonate (or organophosphonic) on metal oxide surface[4] (strategy ***a***, scheme 1) and ii) the one-pot co-condensation of organophosphonate-to-metal alkoxide,[5] resulting in the spontaneous formation of a solid metal oxide in which the walls are uniformly embedded with the organomodifier (strategy ***b***, scheme 1). While the first method affords more stable coating,[4] these materials suffer from the inhomogeneous distribution of the grafting and significant pore clogging because of the tendency of the organic to stack at the pore entrance. The co-condensation method[5] offers best distribution both on the walls and within the pores and more flexibility for engineering titanium dioxide texture (crystallinity and multimodal porosity), owing to the possibility to couple the templating and the sol-gel processes, instantanously.[6,7]

Despite the wealth of synthetic methods available for organophosphonate-bridged-titanium oxide, no report on the open literature has disclosed the co-condensation of two (or more) organophosphonate precursors with soluble titanium species (strategy ***c***, scheme 1). Such rational design, well-optimized for silica-based materials, allowed access to unique properties arising from the precise location of reactive groups in different positions (inter-surface *versus* outer- surface and

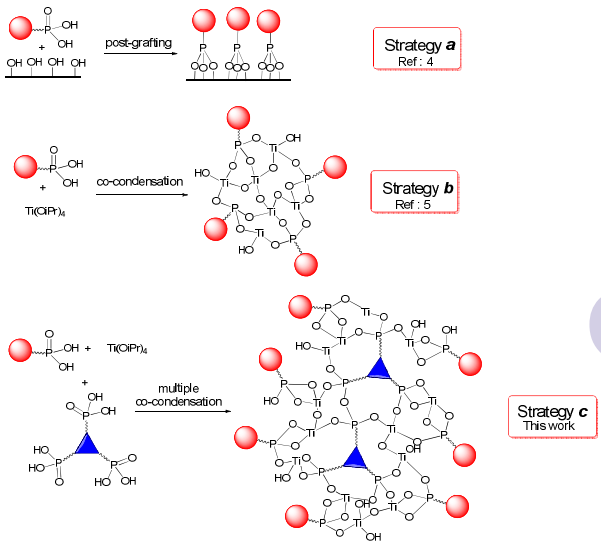


**Scheme 1.** Different strategies adopted (strategy *a* and *b*) or envisioned (strategy *c*) for the preparation of organophosphonate-bridged-titanium dioxide.

[a] *Euromed Research Center, Engineering Division. Euro-Mediterranean University of Fez (UEMF), Fès-Shore, Route de Sidi harazem, Fès, Morocco. a.elkadib@ueuromed.org*
[b] *Université Mohamed V Agdal, Faculté des Sciences Av. Ibn Battouta, BP 1014 and MAScIR fondation, Rabat, Morocco*
[c] *Laboratoire de Chimie de Coordination (LCC) CNRS, 205 route de Narbonne, 31077 Toulouse, France.*

Electronic Supplementary Information (ESI) available: [details of any supplementary information available should be included here]. See DOI: 10.1039/x0xx00000x

pores *versus* walls) and/or by anchoring antagonistic functional groups (acid *versus* base and chelating ligand *versus* hydrophobizing agent) within the restricted nanospace of the material framework.[8] Prompted by these achievements, herein, we validated the approach described in strategy ***c*** by combining two phosphonate-terminated building-blocks and a titania source during the sol-gel mineralisation process.

Our approach is described in Fig. 1. We selected a fourth generation phosphonate-terminated phosphorus dendrimer (denoted herein as **$DG_4$**) as the first organomodifier (96 peripheral phosphonates) and a structure directing agent. We recently evidenced the beneficial effect of using phosphorus dendrimers in the sol-gel medium to generate at a low temperature synthesis, discrete (~5 nm) crystalline anatase nanoparticle entangled in a mesoporous network.[7] These unexpected results emanate from the peculiar topology of the dendrimer substructures (amphiphilic character, swelling behaviour, divergent surface).[9] As a second organomodifier, several units of viologen (both isolated or dendritic) were designed (**$Vio_1$**, **$Vio_2$**, **$Vio_3$**) and functionalized with respectively 1, 3 and 6 phosphonate arms[10] to ensure their covalent anchorage to the metal oxide surface. The choice of the viologen as a specific motif is dictated by its versatile use: photo-activity,[11] electro-redox chemistry,[12] biological response[13] and its well-established stabilizing effect for nano-sized metal particles.[14] Moreover, the synergism of viologen with crystalline titanium dioxide implying electron and energy transfer processes is of paramount importance for the construction of efficient photochromic and electrochromic devices.[15]

The co-condensation has been executed following the strategy denoted herein as path **A** (see below for path **B**, **C** and **D**): under optimized conditions, a phosphonate-terminated fourth generation dendrimer **$DG_4$** was solubilised in an ethanol:water solution (5:2 volume ratio). Then, Ti(O*i*Pr)$_4$ in a 1:20 molar ratio ([terminal organophosphonate] : [Ti]) was added to the transparent dendritic solution at room temperature. Upon addition, the solution became cloudy through polymerisation of the titanium alkoxide precursor. After 15 min of stirring, the third sol-gel precursor (either **$Vio_1$**, **$Vio_2$** or **$Vio_3$**) was added and the resulting solution was heated at 60 °C for 10 hours. After filtration and extensive washing of the precipitate with ethanol, the collected solids were dried at 60 °C for 2 hours given rise to **$M_1$**, **$M_2$** and **$M_3$**, respectively.

The chemical structure of the resulting ternary "dendrimer-viologen-titanium dioxide" systems has been analyzed by

**Table 1**. Textural properties of the as-synthesized multi-functional materials.

| Material | Phosphonate | $S_{BET}$[a] ($m^2.g^{-1}$) | P.D[b] (nm) | P.V[c] (cc/g) | Size[d] (nm) |
|---|---|---|---|---|---|
| $M_1$ | $DG_4$ ; $Vio_1$ | 342 | 3.3 | 0.046 | 5.6 |
| $M_2$ | $DG_4$ ; $Vio_2$ | 360 | 3.5 | 0.124 | 5.5 |
| $M_3$ | $DG_4$ ; $Vio_3$ | 122 | 3.7 | 0.108 | 5.9 |
| $M_4$ | $DG_4$ | 203 | 3.5 | 0.21 | 4.8 |
| $M_5$ | $Vio_2$ | 4[e] | -[e] | -[e] | -[f] |
| $M_6$ | $Vio_3$ | 11[e] | -[e] | -[e] | -[f] |

[a] Specific surface area. [b] Average pore diameter (BJH). [c] Mesoporous volum (BJH). [d] Average crystallite size estimated from the broadening of the {10 reflexion using the Debye–Scherrer equation. [e] Non-porous hybrid material. Amorphous titanium dioxide.

DRIFT and MAS NMR spectroscopies. The presence of C-H vibration band at 2853 and 2913 cm$^{-1}$ indicates the entrapment of organic molecules within the titanium dioxide network (S2a, ESI). The resonance at 1636 cm$^{-1}$ is assignable to C=N vibration. The apparition of a broad band at 1048 cm$^{-1}$, characteristic of P-O-Ti stretching vibration, confirms the covalent anchorage of peripheral phosphonates on the titanium dioxide surface.[3b] The signal at 980 cm$^{-1}$ indicates the presence of the inherently acidic P-OH fragments within the material framework.[3b,6a] More insight has been gained from $^{31}$P and $^{13}$C MAS NMR analyses. Indeed, $^{31}$P MAS NMR displays three signals at ~7 ppm, 16-18 ppm and 60-61 ppm, respectively attributed to the cyclohexaphosphazene core ($N_3P_3$), phosphonate-terminated dendrimer-bridged mineral phase [-P(O)(O-Ti)$_2$] and [-P(O)(O-Ti)(O-H)] on the surface and lastly (-P=S) at the internal branches of the dendrimer framework. Phosphorus signals of the viologen-based additive (**$Vio_x$**) could not be discriminated because of their similarities with those of **$DG_4$** (S3a and Table S2, ESI). However, at this level, it might be ascertained at least the intactness of the dendrimer skeletal during the sol-gel co-condensation process.[7] $^{13}$C CP MAS NMR displays signals typical of **DG** where CH=NH, N-CH$_3$ and CH-OH resonate at ~137, 30, 71 ppm respectively and the aromatic rings are observable at 121, 131 and 150 ppm. The presence of a new signal at 62-63 ppm assignable to CH$_2$-N$^+$ confirms the successful incorporation of the viologen motifs[10] within the solid tectonic network (S3b and Table S2, ESI).

Textural analyses of the three materials have been performed using a set of complementary analytical tools including nitrogen sorption, X-ray diffraction (XRD), SEM and HRTEM microscopies. The nitrogen sorption profile of these three materials is similar to the one obtained for **$M_4$** using only **DG** and Ti(O*i*Pr)$_4$ as sol-gel precursors (Table 1). The specific

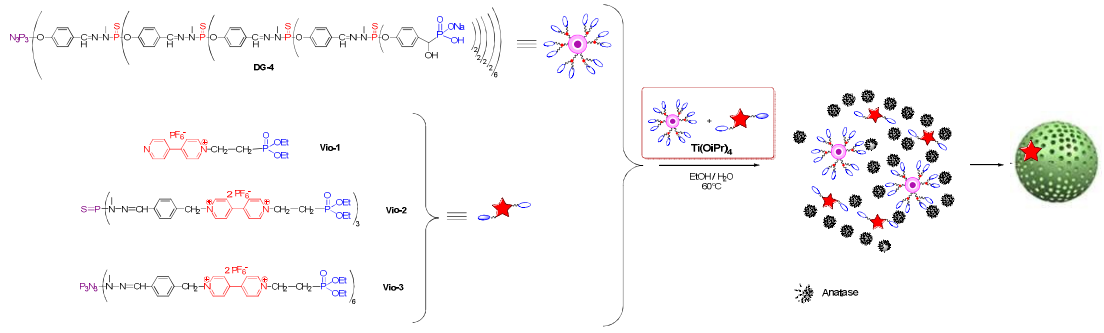

**Fig.1.** General cooperative assembly and sol-gel condensation adopted in the present work.

surface areas were estimated to be 342, 360 and 122 $m^2.g^{-1}$ for **$M_1$**, **$M_2$** and **$M_3$** respectively. Indeed, while a significant enhancement of the opening porosity is obtained with the addition of **$Vio_1$** and **$Vio_2$** (compared to native, viologen-free **$M_4$**: $S_{BET}$ = 203 $m^2.g^{-1}$), the bulky **$Vio_3$** induces a substantial decrease of the specific surface without affecting the pore diameter (D = 3.2, 3.5 and 3.7 nm for **$M_1$**, **$M_2$** and **$M_3$** respectively) (Fig. 2a and Table 1).

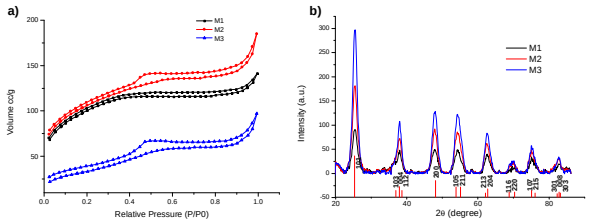


**Fig.2.** a) $N_2$ sorption isotherms and b) Wide angle XRD patterns of **$M_1$**, **$M_2$** and **$M_3$**.

SEM analysis corroborates the openness of the material framework and reveals the presence of spherical aggregates, less-homogeneous and randomly disordered network (Fig. 3a-c). XRD and HRTEM were conjointly performed aiming to get more insight of the nanoscale order and the state (crystalline or amorphous) of the material framework. Similarly to their parent, viologen-free **$M_4$**, the three materials exhibit well-distinguished peaks at 2$\vartheta$ values corresponding to the planes of the crystalline anatase phase (Fig. 2b). The crystal size is estimated to be 5.6, 5.5 and 5.9 nm for **$M_1$**, **$M_2$** and **$M_3$**, respectively (Table 1). These values are slightly superior to that obtained for viologen-free, parent material **$M_4$**, being equal to 4.8 nm. The formation of these small crystalline anatase particles indicates that the presence of the viologen additives (**$Vio_x$**) in the sol-gel medium do not induce any undesirable effect against the early crystallisation reached by the use of phosphorus dendrimer.[7] Moreover, the pivotal role played by phosphorus dendrimer (**$DG_4$**) has been substantiated by comparison with the two hybrid materials prepared by a dendrimer-free route, using solely viologen additives (**$Vio_2$** or **$Vio_3$**) and a titanium alkoxide as sol-gel precursors (**$M_5$** and **$M_6$** in Table 1). These isolated viologen-based phosphonate-embedded titanium dioxide hybrid materials are devoid of both a porous network and a crystalline phase (Table 1). These results confirm again the mandatory presence of **$DG_4$** for ensuring the crystal growth of crystalline anatase from the colloidal solution and for tuning the mesostructure.[7] From HRTEM analyses, discrete crystalline particles are visible throughout the specimen and are aligned along together to form linear, one-dimensional twisted crystalline network. A closer view indicates the presence of lattice fringes and reveals clearly an inter-distance of 0.35 nm assignable to [101] plan (Fig. 3d-f and S4, ESI). Selected-area electron diffraction (SAED) patterns are shown in the onset of each figure and reveal the presence of well-defined diffraction spots characteristic of crystalline anatase nanoparticles (Fig. 3d-f). Similar anisotropic nanostructures have been previously reported using Trizma [2-amino-2-(hydroxymethyl)-1,3-propanediol $(HOCH_2)_3$-$NH_2$], a tridentate cationic ligand as a surface modifier and an assembling agent in the presence of $TiCl_4$ and benzyl alcohol as a sol-gel medium.[16] Through accurate mechanistic studies, it has been concluded that the selective Trizma binding to all crystal planes - except the [001] - provides the driving force for the oriented attachment of the seeded nanoparticles in a linear direction. Herein, the absence of such anisotropic structures in the reference experiments without viologen (Preparation of **$M_4$**) suggests a similar interplay between cationic viologen motifs with the Ti-OH surface of the growing oxo-cluster particles.[16]

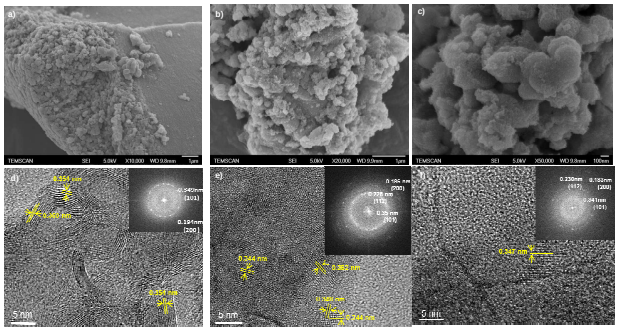

**Fig.3** Microscopic SEM (a-c) and HRTEM (inset: SAED) (d-f) analysis of **$M_1$** to **$M_3$**. a-c, from left to right: **$M_1$**, **$M_2$** and **$M_3$**.

DRUV analyses were undertaken in order to further confirm the presence of photo-active viologen within the material framework. The presence of the adsorption band at 220 nm typical of the 4-4'-bipyridinium units constitutes the most salient evidence for the successful incorporation of the viologen fragments within these tectonic mesostructures (S. ESI). It should be noted that end-capping of anatase nanoparticulates by viologen-terminated phosphonate organic groups accounts for their easy dispersion, which may open new opportunities for processing as reactive thin films or spray dried microspheres.

Having ascertained the covalent linkage of the viologen units within the dendrimer-titanium dioxide network, we further investigated some experimental variants to assess their influence on the textural organization of the material network (Path **B, C** and **D**). Taking however in consideration the necessary presence of **$DG_4$** in the initial stage of the sol-gel mixture to generate crystalline anatase particles, this has not been altered. Indeed, Path **B** consists in introducing all the involved precursors at the same time (without any induction time for coupling **$DG_4$** and $Ti(OiPr)_4$: for comparison, in path **A**, the induction time is of 15 min) and gentle heating of the gel mixture at 60°C for 10 hours. Path **C** consists in the same protocol with heating at 100°C to further consolidate the network. Lastly, path **D** consists in further extending the induction time of coupling **$DG_4$** and $Ti(OiPr)_4$ for 4 hours (rather than 15 min in path **A**) and gentle heating at 60°C for 10 hours. Whatever the protocol used (S1, ESI), hybrid materials in which **$DG_4$**, viologen and crystalline anatase were entangled in mesoporous microspheres were obtained (S6, ESI). The specific surface areas range from 155 to 63 $m^2.g^{-1}$ and the pore diameter almost centred at 3.6 nm (S7 and Table S1, ESI). The nanosized crystalline anatase particles are slightly expanded

(compared to $\mathbf{M_4}$) reaching values around 6.8 and 8.2 nm (S8 and Table S1, ESI).

The presence of the cationic viologen units within the materials framework prompted us to investigate their ability to disperse and stabilize smaller gold nanoparticles.[14] Recently, excellent molecular recognition of viologen-based dendritic macromolecular asterisks for molecular [$HAuCl_4$] gold has been evidenced. Their powerful ability to stabilize smaller gold particles [$Au^0$] for an extended period of eight months without any noticeable aggregation or chemical alteration makes them excellent "reservoir" to store and deliver metallic nanoparticles.[14a] Similarly herein, $\mathbf{M_1}$, $\mathbf{M_2}$ and $\mathbf{M_3}$ hybrid materials were confronted to molecular $HAuCl_4$ followed by $NaBH_4$ reduction (S1, ESI). Upon contacting solution, the initial yellow colour turned into purplish red indicating the formation of gold nanoparticles (Onset of Fig. 4).[17] DRUV analysis shows the typical plasmonic absorption band at 532 nm associated to the presence of gold nanoparticles (S9, ESI).[14]

HRTEM analysis reveals dark spots corroborating the successful formation of ~7 to 8 nm gold nanoparticles (Fig. 4). Assuming that the pore dimensions of these materials do not exceed 3.6 nm, the viologen units seems to be located in the external pore surface where enough space is available for gold expansion upon $NaBH_4$ reduction. Considering the weakness of viologen-gold interactions, these systems seem to be promising as a "release and catch" catalytic materials.

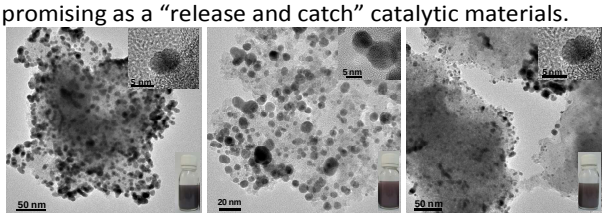


**Fig.4** HRTEM images of respectively from left to right: $\mathbf{M_2}$-**Au** and $\mathbf{M_3}$-**Au** (prepared following path A) and $\mathbf{M_1}$-**Au** (path B).

Herein, an entry to mesoporous multifunctional crystalline organophosphonate-bridged-titanium dioxide hybrid materials has been reported. These fused tectonic nanostructures are built in a synergistic manner: i) $\mathbf{DG_4}$ allows to boost the crystallisation from the colloidal solution and for tuning the mesostructure, ii) titanium-oxo-species act as *in situ* anchoring surface for various phosphonate-terminated building-blocks and iii) viologen acts as a "discrete assembler" for the preferential attachment of anisotropic anatase phase and after, brings its photo-activity and stabilizing effect for [Au°] nanoparticles. Expanding this strategy to cooperative catalytic motifs and bio-machinery systems is currently under active investigation.

1. a) J. Goura and V. Chandrasekhar, *Chem. Rev.*, 2015, **115**, 6854-6965; b) K. J. Gagnon, H. P. Perry and A. Clearfield, *Chem. Rev.*, 2012, **112**, 1034-1054.

2. a) B. C. Jeffrey and W. S. George, *Sol-Gel Science: The Physics and Chemistry of Sol-Gel Processing*, Academic Press Inc edn., Academic Press Inc, 1990.

3. a) T. Y. Ma and S. Z. Qiao, *ACS Catal.*, 2014, **4**, 3847-3855; b) T.-Y. Ma, L. Liu, Q.-F. Deng, X.-Z. Lin and Z.-Y. Yuan, *Chem. Commun.*, 2011, **47**, 6015-6017.

4. a) R. Boissezon, J. Muller, V. Beaugeard, S. Monge and J. . Robin, *RSC Adv.*, 2014, **4**, 35690-35707; b) G. Guerrero, J. G. Alauzun, M. Granier, D. Laurencin and P. H. Mutin, *Dalton Trans.*, 2013, **42**, 12569-12585; c) C. m. Queffélec, M. Petit, P. Janvie , A. Knight and B. Bujoli, *Chem. Rev.*, 2012, **112**, 3777-3807; d) H. Mutin, G. Guerrero and A. Vioux, *J. Mater. Chem.*, 2005, **15**, 3761-3768.

5. a) P. H. Mutin, G. Guerrero, J. G. Alauzun, *J. Ceram. Soc. Japan*, 2015, **123**, 709-713; b) T. Y. Ma and Z. Y. Yuan, *ChemSusChem*, 2011, **4**, 1407-1419.

6. a) A. Dutta, A. K. Patra, S. Dutta, B. Saha and A. Bhaumik, *J. Mater. Chem.*, 2012, **22**, 14094-14100; c) T.-Y. Ma, X.-Z. Lin, X.-J. Zhang and Z.-Y. Yuan, *Nanoscale*, 2011, **3**, 1690-1696.

7. a) Y. Brahmi, N. Katir, J. A. M. Agullo, A. Primo, M. Bousmin , J.-P. Majoral, H. Garcia and A. El Kadib, *Dalton Trans.*, 2015, 4 15544-15556; b) Y. Brahmi, N. Katir, M. Ianchuk, V. Colliere, M. Essassi, A. Ouali, A.-M. Caminade, M. Bousmina, J. P. Maj and A. El Kadib, *Nanoscale*, 2013, **5**, 2850-2856; c) Y. Brahmi, N. Katir, A. Hameau, A. Essoumhi, E. M. Essassi, A.-M. Caminade Bousmina, J.-P. Majoral and A. El Kadib, *Chem. Commun.*, 2011, **47**, 8626-8628.

8. a) U. Diaz, D. Brunel and A. Corma, *Chem. Soc. Rev.*, 2013, **4** 4083-4097; b) T. Asefa, M. Kruk, M. J. MacLachlan, N. Coombs, H. Grondey, M. Jaroniec and G. A. Ozin, *J. Am. Chem. Soc.*, 200 **123**, 8520-8530.

9. A. El Kadib, N. Katir, M. Bousmina and J. P. Majoral, *New J. Chem.*, 2012, **36**, 241-255.

10 N. Katir, J. P. Majoral, A. El Kadib, A. M. Caminade, M. Bousmina, *Euro J. Org. Chem.* 2012, 269.

11. P. M. S. Monk, *The Viologens: Physicochemical Properties, Synthesis and Applications of the salts of 4,4'-bipyridine*, John Wiley & Sons, New York, 1998.

12. C. L. Bird and A. T. Kuhn, *Chem. Soc. Rev.*, 1981, **10**, 49-82.

13. a) K. Milowska, J. Grochowina, N. Katir, A. El Kadib, J.-P. Majoral, M. Bryszewska and T. Gabryelak, *Mol. Pharmaceutics*, 2013, **10**, 1131-1137; b) K. Ciepluch, N. Katir, A. El Kadib, A. Felczak, K. Zawadzka, M. Weber, B. Klajnert, K. Lisowska, A.-M. Caminade, M. Bousmina, M. Bryszewska and J. P. Majoral, *Mol. Pharmaceutics*, 2012, **9**, 448-457.

14. a) N. Katir, A. El Kadib, V. Colliere, J. P. Majoral, M. Bousmina, *Chem. Commun.*, 2014, **50**, 6981-6983; b) N. Fattou, C. M. Maroneze, L. P. D. Costa, M. Strauss, I. O. Mazali, Y. Gushikem, *Colloids Surf. A*, 2013, **437**, 120-126.

15. S. Y. Choi, M. Mamak, N. Coombs, N. Chopra, G. A. Ozin, *Nano Lett.*, 2004, **4**, 1231-1235.

16 J. Polleux, N. Pinna, M. Antonietti, M. Niederberger, *Adv. Mater.*, 16, 2004, 436-439.

17 C. Burda, X. Chen, R. Narayanan, M. A. El-Sayed, *Chem. Rev.*, 2005, **105**, 1025–1102.